

Review paper

## Imaging of spinal and central nervous system brucellosis: a review

Sebastian Lipka<sup>1,A,B,E,F</sup>, Radosław Zawadzki<sup>1,A,B,E</sup>, Zeynep Gamze Kilicoglu<sup>2,B</sup>, Joanna Zajkowska<sup>3,B</sup>,  
Urszula Łebkowska<sup>1,A,B</sup>, Bożena Kubas<sup>1,B,E</sup>

<sup>1</sup>Department of Radiology, Medical University of Białystok, Poland

<sup>2</sup>Department of Radiology, VKF American Hospital, Istanbul, Turkey

<sup>3</sup>Department of Infectious Diseases and Neuroinfections, Medical University of Białystok, Poland

### Abstract

Brucellosis is a zoonotic disease caused by Gram-negative bacteria of the *Brucella* genus that can be acquired through contact with a contaminated animal or its secretions. The course of the disease can be acute, chronic, or persistent. Axial skeleton and central nervous system (CNS) are among the most common affected locations and may be involved in each of the forms. Due to the varying clinical picture of the disease, diagnosis is made mainly on the basis of laboratory examinations that detect specific IgM and IgG antibodies in blood or other biological material and/or cultures. Imaging methods, especially magnetic resonance imaging, can aid in establishing proper diagnosis, monitoring of the disease and, to some extent, enable differential diagnosis before obtaining the laboratory tests results. The aim of this review is to present imaging features of *Brucella* infection of the spine and CNS and provide the recent advancements in the field.

**Key words:** spinal brucellosis, neurobrucellosis, computed tomography, magnetic resonance imaging, neuroimaging.

### Introduction

Brucellosis, the most common infectious zoonosis, is becoming a significant healthcare concern, especially in less developed countries. The annual incidence is estimated at about 2.1 million cases [1]. The distribution of cases in the world is not uniform – most cases are recorded in the intertropical zone of Africa and Asia, but the risk of disease in the temperate zone, although lower, is not negligible. The disease is caused by Gram-negative bacteria of the *Brucella* genus, the main reservoir of which are farm animals: sheep, goats, pigs, dogs, and rats. Infection can occur through direct contact with an infected animal and its secretions; consumption of raw or unpasteurised dairy and dairy products from infected animals; and by inhalation in the case of people working in meat processing, research laboratories, and health care facilities or indirectly

through contact with infected surfaces. There are also reports of transplacental transmission of infection [2].

The clinical presentation of brucellosis is not characteristic and depends on many factors, including the species of bacteria, the size of the infective dose, the route of infection, and the immunological status of the host. Usually, symptoms appear after an incubation period of 5 days to 6 months. There are acute, chronic, and persistent forms of brucellosis. In each of them, any system and organ can be involved, but most often the musculoskeletal system, the nervous system (neurobrucellosis), the genitourinary system, and the liver are affected.

In the musculoskeletal system, infection can manifest as mono- or polyarthritis and osteomyelitis of the spine. Central nervous system (CNS) infection presents as lymphocytic meningitis and/or encephalitis, myelitis, brain and/or epidural abscesses, peripheral neuropathy, damage

### Correspondence address:

Sebastian Lipka, Department of Radiology, Medical University of Białystok, 24A M. Skłodowskiej-Curie St., 15-276 Białystok, Poland,  
e-mail: [lipkasebastian5@gmail.com](mailto:lipkasebastian5@gmail.com)

### Authors' contribution:

A Study design · B Data collection · C Statistical analysis · D Data interpretation · E Manuscript preparation · F Literature search · G Funds collection

to the cranial nerves, or symmetric damage to the VIII cranial nerve [3].

Due to the rich symptomatology and the multitude of clinical manifestations, diagnosis of brucellosis is difficult, especially in non-endemic regions and in the absence of a history of exposure to pathogens. Serological tests (enzyme-linked immunosorbent assay [ELISA], Rose Bengal, Coombs test) detecting specific IgM and IgG antibodies in blood serum remain the basis for diagnosing brucellosis. Additional diagnostic methods include cultures of biological material such as blood, cerebrospinal fluid, bone marrow, and synovial fluid; detection of genetic material of bacteria by polymerase chain reaction (PCR), and skin tests with brucellin – the so-called Burnet test. Due to the insufficient sensitivity and specificity of the above-mentioned methods [4], as well as the long incubation time of cultures, making a final diagnosis and implementing appropriate treatment is delayed, which poses a higher risk of complications for the patients. Therefore, in patients presenting with findings suggestive of brucellosis, especially of the nervous system and axial skeleton, multifaceted laboratory and imaging diagnostics is important.

In cases of suspected brucellosis, imaging methods are used in differential diagnosis, to assess the response to treatment and monitor disease complications.

### Imaging in spondylodiscitis

It is proposed that spine infections can occur in 3 ways: through hematogenous spread of pathogens from distant foci, as a direct infection of the surgical site, and through continuity with adjacent tissues or structures, e.g. muscles or pelvic organs [5].

There are several theories explaining the predilection in infecting a specific region of the spine by infectious agents. One of them draws attention to the structure of the spine arterial blood supply from the anterior and posterior vertebral arteries – it is believed that bacterial embolism occurs in the arterial microcirculation of the endplates of the vertebral bodies. Another theory claims that pathogens can reach the vertebral structures through reflux from the pelvic venous plexus, which may explain the “preference” to affect the lumbar region [5].

In a retrospective study by Andriopoulos *et al.* [6] involving a group of 144 patients with confirmed acute brucellosis, spine involvement was observed in 41 patients, and in 2 patients vertebral body inflammation with neurological symptoms occurred.

In a Turkish prospective study [7] including 251 patients with diagnosed brucellosis, 26 showed signs of spondylodiscitis. Eight patients developed a paravertebral or epidural abscess, but none of the patients had posterior vertebral involvement or subligamentous spread. Fifteen cases involved the lumbar spine, 6 thoracic spine, 4 thoracic and lumbar spine, and one patient had cervical spine involvement. In addition, in 3 patients with thoracic spine invol-

vement, there was a vertebral body destruction complicated with compression of the spinal cord and nerve roots.

Retrospective study by Turgut *et al.* [8] including an analysis of 452 cases of spinal brucellosis proved that 46% of patients had involvement of the lumbar spine, while in most patients (92%) the infection radiologically presented as spondylitis or spondylodiscitis. The most common changes in X-ray, computed tomography (CT), and magnetic resonance imaging (MRI) included narrowing of the intervertebral spaces, destruction of the vertebral body, sclerosis, or lytic changes of the vertebral endplates. In 16.7% of patients, MRI revealed a paravertebral inflammatory infiltrate or abscess, while in 15.1% of cases epidural abscesses developed.

In a retrospective study by Varikkodan *et al.* [9] conducted on a group of 346 patients with laboratory-confirmed brucellosis, spine involvement occurred in 29 (8.4%) patients, and 6 patients developed symptoms of meningitis. In the analysis of 1590 cases of brucellosis conducted by Liu *et al.* [10] spinal involvement was reported in 29.49% of patients, while 0.82% of patients presented symptoms of meningitis.

Table 1 summarises the epidemiological and clinical data from selected publications.

Radiological signs of infection of the intervertebral disc and the endplates of the adjacent vertebral bodies usually become visible 3 to 5 weeks after the onset of clinical symptoms [17]. There are 2 forms of spinal infection: localised, limited to the anterior aspect of the endplates of the vertebral body, and disseminated, where the disease involves the vertebral body, intervertebral disc, adjacent vertebrae, epidural space, meninges, and spinal cord [17,18].

Classic radiography of the spine in lateral and AP projections, as a commonly available examination, is usually performed first. The most common findings include erosions of the anterior aspect of the lower or upper endplate, narrowing of the intervertebral space, and reactive osteophyte formation of the anterior aspect of the endplates, referred as the “parrot’s beak” sign. Vacuum sign secondary to ischaemic changes is observed less frequently [17,18].

Earlier visualisation of pathological changes is possible with CT, in which the affected intervertebral discs appear hypodense compared to the unaffected spine section. In addition, flattening of the discs and inflammatory changes in the endplates can be observed earlier than in the radiographic examination [17].

Magnetic resonance imaging is the method of choice in diagnosing spinal involvement, due to its high sensitivity (96%) and specificity (94%) [19], especially in the early stages of the disease. It also provides good visualisation of the surrounding tissues and the spinal canal structures involvement. The examination protocol should include at least 3 sequences: T1-weighted, T2-weighted, and T1-weighted after the administration of a contrast agent [5].

In the early stage of the disease, bone marrow oedema of the vertebral body occurs, which is characterised by low

**Table 1.** Clinical manifestations and complications of axial skeleton brucellosis

Factor		Turunc <i>et al.</i> [11]	Shi <i>et al.</i> [12]	Varikkodan <i>et al.</i> [9]	Sawafi <i>et al.</i> [13]	Liu <i>et al.</i> [10]	Andriopoulos <i>et al.</i> [6]	Pourbagher <i>et al.</i> [7]	Turgut <i>et al.</i> [8]	Solera <i>et al.</i> [14]	Lu <i>et al.</i> [15]	Gou <i>et al.</i> [16]
Number of cases		32	880	346	57	1590	144	251	452	285	167	615
Sex, <i>n</i>	M	19	672	299	34	1146	93	180	–	–	136	485
	F	13	238	47	23	444	51	71	–	–	31	130
Median age (years)		59.0 ± 13.9	50 ± 8	39.62 ± 15.05	6.0 ± 3.8	47.3	–	45	–	–	52.29 ± 9.46	53.05 ± 11.06
Clinical manifestation, <i>n</i>	Spondylodiscitis/Spondylitis	32	146	–	–	469	44	26	264	35	–	615
	Sacroiliitis	–	24	–	–	–	9	71	–	32	–	–
	Epidural/Paravertebral abscess	–	44	–	–	–	–	8	90	31	–	266/313
	Encephalitis	–	–	–	–	1	–	–	–	–	–	–
	Arthritis with spondylitis	–	–	–	–	337	–	–	–	–	–	–
	Meningitis	–	–	6	–	13	–	–	–	–	–	–
	Arthritis	–	264	11	–	989	–	–	–	18	–	–
	Intramedullary mass	–	–	–	–	–	–	–	3	–	–	–
Lesion spinal region, <i>n</i>	C	1	–	–	–	–	–	1	21	1	15	16
	C-Th	–	–	–	–	–	–	–	–	2	–	2
	Th	10	–	–	–	–	–	6	43	0	5	35
	Th-L	–	–	–	–	–	–	–	6	0	2	8
	C-Th-L/C-Th-L-S	–	–	–	–	–	–	–	–	–	1	40
	L	21	–	–	–	–	–	15	207	23	142	397
	S	0	–	–	–	–	–	–	1	1	2	3
	L-S	–	–	–	–	–	–	–	27	8	–	114

M – male, F – female, C – cervical spine, Th – thoracic spine, L – lumbar spine, S – sacral spine, (–) not stated

signal intensity in T1-weighted images, and high signal intensity in T2-weighted images and in the fluid attenuated inversion recovery (FLAIR) sequence. Short tau inversion recovery (STIR), T2 with fat saturation (FatSat), or spectroscopic inversion recovery sequences allow detection of changes at a very early stage of advancement [18,20]. Subsequently, osteolysis of the anterior aspect of the upper endplate of the vertebral body occurs at the disc-vertebral junction. Inflammatory and regenerative processes coexist, which is reflected by productive changes of the edge of the vertebral body (X-ray sign of “parrot’s beak”) and areas of subchondral sclerosis [21]. The vertebral body itself is usually not affected. Affected vertebral bodies, endplates, and facet joints show post-contrast enhancement in fat-saturated T1-weighted images [20]. This phenomenon is particularly important in cases where there is no severe bone marrow oedema [19]. Although the findings in the course of spinal brucellosis are characteristic, differen-

tial diagnosis may be difficult in patients with a history of spinal trauma, degenerative disease, previous spine surgery, neoplastic processes involving the spine, or with coexisting haematological diseases. In such situations, diffusion-weighted imaging (DWI) sequences are useful, in which the “claw sign” can be observed, i.e. marked boundaries between areas of vascularised and unchanged bone marrow of 2 adjacent vertebral bodies resembling a claw, which suggests a degenerative background of the observed changes, while its absence suggests an infectious background [18,19].

Intervertebral disc involvement is observed after the vertebral body becomes infected. Morphologically, it presents as the disc oedema characterised by high signal intensity in T2-weighted images and STIR sequences and shows significant contrast enhancement in T1-weighted sequences. In the case of severe oedema, a circular protrusion may form, mimicking the early stage of interver-

tebral disc herniation. Infection may lead to destruction of the vertebral body with subsequent herniation of the disc contents into the vertebral body and the formation of an intravertebral hernia. In spinal brucellosis, a “vacuum sign” is observed, i.e. a small amount of gas contained between the intervertebral disc and the infected upper endplate. This sign is characterised by low signal intensity in all MR sequences. In the later stage of the disease, there is a slight narrowing of the intervertebral space [17,18].

Paravertebral abscesses in the course of brucellosis are rare (up to 30% of cases [17]), do not show aetiology-specific features in MRI, and may present with various annular patterns of contrast enhancement. Involvement of paravertebral tissues manifests as increased signal intensity, and blurring of muscle and fat tissue outlines in T2-weighted images [18].

Figures 1 and 2 demonstrate typical changes in spinal brucellosis.

The inflammation can spread to the epidural space with or without spinal cord compression. In brucellosis, epidural abscesses most often develop through continuity with adjacent spinal regions. Dissemination from paravertebral tissues and direct infection by penetrating trauma or surgical procedures are also reported. When infection

occurs via the bloodstream, the surrounding spinal structures remain unchanged. Epidural abscesses in brucellosis do not show specific features on MRI; similarly to abscesses of other aetiologies, they take on the shape of a “curtain sign”, which is best appreciated on T2-weighted and T1-weighted images with fat saturation after contrast administration. The extent of the disease is assessed based on T1-weighted images before and after contrast administration in the axial and sagittal planes. The intensity and pattern of post-contrast enhancement plays a major role in the diagnosis – epidural abscesses containing fluid and necrotic tissue show an annular type of post-contrast enhancement, whereas phlegmon that does not contain fluid elements is characterised by a diffuse pattern of enhancement. Due to the different therapeutic approach, it is always necessary to differentiate abscess from phlegmon on MRI [18].

There is no widely accepted classification of morphological changes observed in spinal brucellosis imaging studies. Based on the analysis of MRI studies of the spine of 615 patients with laboratory-confirmed brucellosis, Gou *et al.* [16] proposed a 5-stage classification of spinal pathology reflecting the pathophysiological background, different therapeutic approach, and prognosis. Type I, called early, includes cases in which only bone marrow

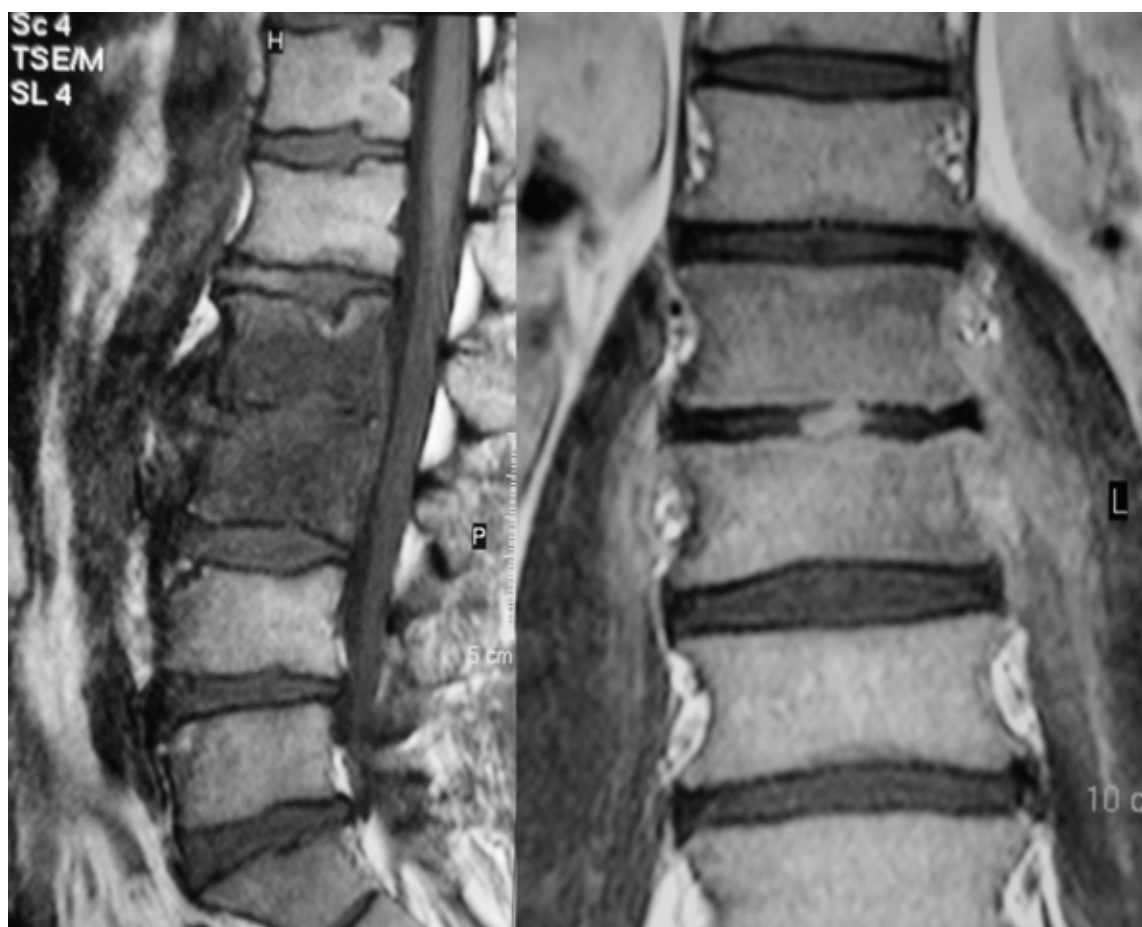


**Figure 1.** *Brucella* spondylitis. Sagittal (left) and coronal (right) T1-weighted magnetic resonance images show bone marrow oedema of the L2-L3 vertebrae, intervertebral space involvement, formation of prevertebral abscess, and bilateral psoas muscles infiltrate [Courtesy of Zeynep Gamze Kilicoglu, MD, Assoc. Prof. of Radiology, Department of Radiology, VKF American Hospital, Istanbul]



**Figure 2.** Axial contrast-enhanced (upper) and pre-contrast (lower) T1-weighted fat-sat magnetic resonance images show perivertebral infiltration [Courtesy of Zeynep Gamze Kilicoglu, MD, Assoc. Prof. of Radiology, Department of Radiology, VKF American Hospital, Istanbul]

oedema of the vertebral bodies is observed, with or without concomitant oedema of the perivertebral tissues, showing low signal intensity on T1-weighted images and high signal intensity on T2-weighted images. In this group, conservative treatment can be successfully implemented. In type II lesions disease progression and destruction of the vertebral bodies occur, coexisting with repair processes, but remain dominant. Depending on the extent of the destructive processes, type II is further divided into type IIa, b, and c. Type IIa is characterised by the destruction of 1/3 of the endplate of the vertebral body with preserved vertebral body height and no abscesses. Most patients with this type can be treated conservatively; if there is no response, surgical treatment is considered. Destruction of more than 2/3 of the endplate with preserved vertebral body height is classified as type IIb. Additionally, in type IIc the vertebral body is compressed. Treatment of types IIb and IIc lesions includes conservative treatment, and minimally invasive and

classical surgical methods. Type III represents lesions in which reparative changes predominate. In MRI, the lesions demonstrate homogeneously/heterogeneously low signal intensity in T1- and T2-weighted sequences and have sclerotic edges. This group usually does not require therapeutic interventions.

Nuclear medicine examinations, such as  $^{67}\text{Ga}$  single photon emission computed tomography ( $^{67}\text{Ga}$ -SPECT) or  $^{99\text{m}}\text{Tc}$ -methyl diphosphonate ( $^{99\text{m}}\text{Tc}$ -MDP), due to low specificity, are not routine modalities used in the diagnosis of infectious diseases of the spine. Promising results have been obtained in fluorodeoxyglucose (FDG)-positron emission tomography (PET), which allows the differentiation of infectious changes from degenerative or traumatic changes that do not cause increased FDG uptake. Currently, it is believed that nuclear medicine methods should be reserved for cases where the diagnosis is uncertain or other modalities (including MRI) are inconclusive [19,20].

## CNS imaging

Meningitis in the course of brucellosis is rare (1.7-10% [22]). T1-weighted and FLAIR sequences show a blurred boundary between the cerebrospinal fluid and the spinal cord, loss of the spinal cord outline, and increased meningeal signal, which reflects damage of the blood-brain barrier, changes in the cerebrospinal fluid composition, and thickening of the meninges. In the later stages, cerebrospinal fluid circulation is disturbed, which, in combination with the previously mentioned factors, can lead to the formation of adhesions, inclusions, and even thickening of the nerve roots in more advanced cases. In the early stages of the disease, morphological changes can be discrete, so in the case of suspected infectious meningitis, the MRI protocol should include post-contrast sequences, which allow for the detection of small changes. The earliest changes detectable in imaging studies are linear or nodular enhancement of the meninges and nerve root sheaths. It should be remembered that these symptoms are not specific for *Brucella* infection and require differential diagnosis with subarachnoid haemorrhage, meningeal metastases, sarcoidosis, and Guillain-Barré syndrome, and may also be seen in patients after lumbar puncture. As a result of impaired circulation of cerebrospinal fluid, there is a redistribution of fluid flow through the central canal of the spinal cord, which may lead to the formation of intracanalicular cysts, which, when combined, lead to the formation of syringomyelia. Other complications include inflammation and thrombosis of the vessels of the pia mater, ischaemia, and infarction of the spinal cord [18].

Myelitis is not a common manifestation of *Brucella* infection. Spinal cord involvement may occur as a result of various mechanisms: direct infection of the spinal cord with symptoms of inflammation and abscess formation; as a result of immunological reactions presenting as acute disseminated encephalomyelitis or acute inflammatory polyneuropathy; or myelopathy due to septic emboli or venous thrombosis. MRI of the spinal cord in the acute phase of the disease may be normal or nonspecific. In T2-weighted images, mild oedema of the spinal cord is visible as poorly demarcated areas of increased signal, while areas of low signal intensity may correspond to forming granulomas. In the subacute phase diffuse, patchy and annular areas of contrast enhancement are observed, corresponding to significant spinal oedema and abscesses in various stages of evolution. Multiple sclerosis and metastatic neoplasms should be considered in the differential diagnosis [3,18].

There are few data in the literature on imaging of neurobrucellosis. Al-Sous *et al.* [23] attempted to characterise the patterns of CNS involvement observed in imaging studies and to determine the correlation between observed abnormalities and clinical symptoms in patients with laboratory-confirmed brucellosis. Based on the MRI studies of 23 patients (17 CNS studies, 6 spine studies) and brain CT studies of 23 patients, 4 groups of imaging findings were distinguished, which are supposed to reflect

the pathophysiology and clinical symptoms observed in patients: no detectable changes, inflammatory changes, white matter changes, and vascular changes. Inflammatory changes in imaging studies are characterised by contrast enhancement of the meninges, perivascular spaces, lumbar nerve roots, or inflammatory granulation tissue formation. In this group, complete remission of disease symptoms (headaches, optic disc oedema, epileptic seizures, polyradiculopathy, or lymphocytic meningitis) was achieved after treatment. In the third group, different types of T2-hyperintense white matter areas distribution were observed: periventricular, diffuse with a predilection for arcuate fibres, and localised resembling demyelinating changes. It is stated that the described changes have an autoimmune background. The group of patients with vascular changes included cases where subthalamic haemorrhage or silent clinical areas of lacunar infarction of the basal ganglia were observed in CT and/or MRI. The authors suggest inflammation of small vessels as the cause of vascular changes in the course of brucellosis.

Jafari *et al.* [24] reported a series of 7 cases of brucellosis complicated by meningitis. Imaging studies showed contrast enhancement of the meninges, dilatation and tortuosity of the optic nerves, and multiple demyelinating foci located in the subcortical and periventricular white matter.

Yazdi *et al.* [25] described a case of a 61-year-old female patient diagnosed with brucellosis who developed neurological complications during treatment. MRI revealed focal hyperintense lesions in T2-weighted sequences and contrast-enhancement in T1-weighted sequences, located bilaterally in the upper cerebellar peduncles. Additionally, small hyperintense lesions in T2-weighted images were visualised in the pons and midbrain with a patchy pattern of post-contrast enhancement. Spine imaging revealed diffuse T2-hyperintense lesions, contrast-enhancing, located intraspinally in the C-Th region of the spine, and contrast enhancement of cauda equina.

In rare cases neurobrucellosis can be complicated by ventriculitis. De la Pena-Sosa *et al.* [26] described a case of a 55-year-old farmer diagnosed with *Brucella* meningitis, in whom MRI revealed inflammation of the third and fourth ventricles with suprasellar infiltration, hypothalamitis, and pituitary abscess. The patient clinically presented symptoms of multihormonal hypopituitarism. Alhatou *et al.* [27] documented the case of a 37-year-old shepherd with a history of chronic low-grade fever, weakness, and weight loss, who developed new neurological symptoms. Laboratory tests showed significant titres of antibodies against *B. abortus* and *B. melitensis*, while biochemical results of the cerebrospinal fluid suggested an atypical CNS infection. MRI of the brain and spine showed contrast enhancement of the meninges in the brainstem, and cervical and lumbar spine, and bilaterally in the V, VII, and VIII cranial nerves and the ependymal lining of the ventricular system. The third and fourth ventricles were dilated. The lesions showed a tendency to disappear during the follow-up MRI in the third week of treatment.

## Differential diagnosis

As mentioned, the clinical manifestation of brucellosis is so rich and non-specific that it is called the “great imitator”. Due to the multiple symptomatology and the lack of specific symptoms in CNS imaging studies, differential diagnosis can be very broad and includes conditions such as multiple sclerosis, acute disseminated encephalomyelitis, Lyme disease, infectious CNS inflammation, neurosarcoïdosis, or Guillain-Barré syndrome [23,25]. The correlation of imaging findings with laboratory tests and clinical symptoms is extremely important.

MRI of the spine using the latest techniques and sequences allows for differentiation from degenerative changes, metastatic changes, or haematological diseases. It may be difficult to differentiate brucellosis from other infectious diseases involving the spine and adjacent structures such as of tuberculous, atypical, fungal, or purulent bacteria aetiology, which have in common the long-term culture process with a high risk of false negative results. For these reasons, it is reasonable to attempt to differentiate the aetiology of the observed lesions already at the stage of imaging. The literature draws attention to differences in predilection for affected spine regions; the extent to which the vertebral body is involved; the possibility of involvement of the intervertebral disc, paravertebral tissues, and epidural space; subligamentous spread, or involvement of the posterior structures of the spine, as well as the number and continuity (or lack thereof) of the affected spine vertebrae.

Trunc *et al.* [11] compared clinical, laboratory, and radiological data of patients diagnosed with spondylodiscitis with an underlying tuberculosis, brucellosis, and pyogenic bacterial infection. The study included 13 patients with tuberculosis, 32 patients with brucellosis, and 30 patients with infection by other bacterial species. In the group of patients with brucellosis of the spine, the cervical spine was affected in 3.1% of patients, the thoracic spine in 31.2%, and the lumbar spine in 65.6%, while none of the patients had the sacral spine affected. In the group of patients with tuberculosis, these percentages were 0%, 53.8%, 46.1%, and 0%, respectively. For the other aetiologies, the share was 6.6%, 30%, 60%, and 3.3%, respectively. These results were not statistically significant. The location of pathological lesions in the affected motor segment was also compared, i.e. involvement of the anterior or posterior aspect and the formation of lumbar muscle abscesses. Statistically significant results were achieved for the involvement of the posterior aspect of the motor segment and the tendency to form lumbar muscle abscesses – in the group of patients with brucellosis they were 3.1% and 6.2%, respectively; in the tuberculosis group 61.5% and 46.1%, while in the remaining group 6.6% and 10%.

In the work of Gonzales *et al.* [5] it was noted that infections with purulent bacteria primarily concern the anterior aspect of the vertebral body, and in the late phase

the vertebral body is destroyed with the spread to the adjacent vertebra. The authors distinguished 3 forms of early tuberculous infection: a form with the involvement of the peridisc structures, with the involvement of the adjacent areas of the vertebral bodies through continuity, a form with scalloping of the anterior segments of the vertebral bodies and the formation of large subligamentous abscesses, and primary involvement of the central aspect of the vertebra with its collapse and accompanying “flat vertebra” type deformation without involvement of the structures of the intervertebral space. In case of the spinal brucellosis, a serrated outline of the endplates of the vertebral bodies is more often observed without involvement of the vertebral body. Intervertebral spaces, and paravertebral and epidural tissues, affected to varying degrees, can be observed in all aetiologies except brucellosis [20].

The MRI findings suggesting a tuberculous infection include well-demarcated paravertebral lesions, a thin and smooth abscess capsule, subligamentous spread to 3 or more spinal segments, involvement of multiple vertebral bodies, and annular enhancement of intraosseous abscesses. The following may be suggestive of other aetiologies: poorly demarcated lesions in the paravertebral space, the presence of abscesses with a thick, irregular wall, no subligamentous spread or spread less than 3 vertebral segments, involvement of at most 2 vertebral bodies, and no intraosseous or paravertebral abscesses [20].

In a Chinese study [28] the clinical course and imaging of spinal infections of fungal aetiology and brucellosis were compared. Based on the analysis of 12 patients with fungal spinal infections and 31 cases of spinal brucellosis, a statistically significant difference was found in the location of pathological changes within the spine segment observed in CT and MRI – lesions in the course of brucellosis tend to affect the intervertebral space with concomitant sclerotic reactions of the endplates of the adjacent vertebral bodies. No significant difference was observed in the number of affected spine segments. In the MRI examination, brucellosis lesions were characterised by low signal intensity in T1-weighted images and high signal intensity in T2-weighted images, whereas fungal lesions were characterised by low signal intensity in both T1- and T2-weighted images.

In the era of accelerating progress and wide implementation of artificial intelligence algorithms in medicine, Wang *et al.* [29] attempted to create a machine learning model that helps differentiate between spondylodiscitis of tuberculous aetiology, in the course of brucellosis and inflammation with and without bacteriologically confirmed tuberculosis. Data from 190 patients were used, including the following: age, sex, level of the involved vertebra, involvement of the intervertebral space, size of paravertebral abscesses (no abscess, no obvious signs of abscess in MRI, small abscess, the largest abscess smaller than the adjacent vertebral body, large abscess, abscess larger than the adjacent vertebral body), T1-weighted sagittal MR images of the spine, T2-weighted, and T2-weighted with fat suppress-

**Table 2.** Differential diagnosis of infectious spine diseases [5,16,17,19,20,28]

Involvement of	Brucellosis	Tuberculosis	Pyogenic bacteria	Fungal
Spinal region	Lumbar	Thoracic or thoraco-lumbar junction	Lumbar	Lumbar
Vertebral body	Relatively preserved MR: hypointense on T1-weighted, various T2-weighted signal intensity	Early stage: anterior aspect of the vertebral body; 3 patterns: peridiscal with involvement and the contiguous spread to adjacent vertebral bodies; anterior with the scalloping of the anterior aspect of the vertebral body and formation of subligamentous abscesses; central with collapse of the vertebral body and without involvement of the intervertebral space	Early stage: anterior aspect of the endplates and vertebral body; MR: hypointense on T1-weighted images, hyperintense on T2-weighted images	Serrated outline of vertebral endplates without significant destruction of the vertebral body MR: hypointense on T1- and T2-weighted images
		Late phase: relatively preserved vertebral body MR: variable signal intensity in T1-weighted images reflecting repair processes	Late stage: destruction of the vertebral body with involvement of adjacent vertebral bodies; MR: T2 hyperintense with homogeneous post-contrast enhancement	
Intervertebral space	Present MR: T1 hypointense, T2 hyperintense	Variable: from sparing the intervertebral space to significant destruction	Present: early-stage involvement MR: T2 hyperintensity and enhancement	Typically spared
Paraspinal and/or epidural space	Typically not present, lack of paraspinal abscess	Large paraspinal abscesses (up to 75% of patients) with thin and smooth annular contrast enhancement	Inflammatory changes and/or small abscesses with a thick and irregular, enhancing rim	Small paraspinal abscesses thick and irregular rim enhancement
Posterior spinal structures	Typically not involved	Can be involved	Typically not involved	Can be involved, including the rib heads
Anterior subligamentous spread	Typically not present	Present, may be more extensive than the changes in the vertebral body	Uncommon	Common
Adjacent vertebrae	Uncommon	Present, significant destruction of bone	Present, destruction of the endplates of the adjacent vertebrae	Uncommon
Multiple vertebral segments	Uncommon	Common, skip lesions	Uncommon	Common, skip lesions

sion. Using the model, a statistically significant difference was obtained between the groups with confirmed brucellosis and tuberculosis in terms of the involvement of the inflammatory process in the intervertebral space and the size of paravertebral abscesses. No statistically significant differences were observed in the predilection of infectious agents for specific spine regions. In turn, Chen *et al.* [30] built a deep learning model that allows for accurate differentiation of tuberculosis and brucellosis of the spine based on MRI examinations, which performed better than a team of 2 radiologists.

Table 2 summarises features useful in the differential imaging diagnosis of spinal infections.

## Conclusions

Diagnostics of brucellosis is multimodal, mainly based on clinical picture, and serological and microbiological testing. Imaging modalities, especially CT and MRI, enable

a faster diagnosis and implementation of appropriate treatment, consequently reducing the risk of complications. In the case of axial skeleton involvement, the diagnosis of brucellosis may be indicated by the location of lesions in the lumbar spine, a predilection to the anterior aspect of the endplate with relatively minor involvement of the vertebral body, a lack of tendency to form paravertebral abscesses, or involvement of a single motor unit of the spine. In the case of CNS brucellosis, the literature does not indicate specific findings in imaging, which often do not correlate with the clinical picture and complaints reported by patients, and the diagnosis is based mainly on serological testing.

## Disclosures

1. Institutional review board statement: Not applicable.
2. Assistance with the article: None.
3. Financial support and sponsorship: None.
4. Conflicts of interest: None

## References

- Laine CG, Johnson VE, Scott HM, Arenas-Gamboia AM. Global estimate of human brucellosis incidence. *Emerg Infect Dis* 2023; 29: 1789-1797.
- Qureshi KA, Parvez A, Fahmy NA, Abdel Hady BH, Kumar S, Ganguly A, et al. Brucellosis: epidemiology, pathogenesis, diagnosis and treatment – a comprehensive review. *Ann Med* 2023; 55: 2295398. DOI: 10.1080/07853890.2023.2295398.
- Kizilkilic O, Calli C. Neurobrucellosis. *Neuroimaging Clin N Am* 2011; 21: 927-937.
- Freire ML, de Assis TSM, Silva SN, Cota G. Diagnosis of human brucellosis: systematic review and meta-analysis. *PLoS Negl Trop Dis* 2024; 18: e0012030. DOI: 10.1371/journal.pntd.0012030.
- Gonzalez GA, Porto G, Tecce E, Oghli YS, Miao J, O'Leary M, et al. Advances in diagnosis and management of atypical spinal infections: a comprehensive review. *N Am Spine Soc J* 2023; 16: 100282. DOI: 10.1016/j.xnsj.2023.100282.
- Andriopoulos P, Tsironi M, Deftereos S, Aessopos A, Assimakopoulos G. Acute brucellosis: presentation, diagnosis, and treatment of 144 cases. *Int J Infect Dis* 2007; 11: 52-57.
- Pourbagher A, Pourbagher MA, Savas L, Turunc T, Demiroglu YZ, Erol I, et al. Epidemiologic, clinical, and imaging findings in brucellosis patients with osteoarticular involvement. *Am J Roentgenol* 2006; 187: 873-880.
- Turgut M, Turgut AT, Koşar U. Spinal brucellosis: Turkish experience based on 452 cases published during the last century. *Acta Neurochir (Wien)* 2006; 148: 1033-1044.
- Varikkodan I, Naushad VA, Purayil NK, Zahid M, Sirajudeen J, Ambra N, et al. Demographic characteristics, laboratory features and complications in 346 cases of brucellosis: a retrospective study from Qatar. *IJID Regions* 2024; 10: 18-23.
- Liu B, Liu G, Ma X, Wang F, Zhang R, Zhou P, et al. Epidemiology, clinical manifestations, and laboratory findings of 1,590 human brucellosis cases in Ningxia, China. *Front Microbiol* 2023; 14: 1259479. DOI: 10.3389/fmicb.2023.1259479.
- Turunc T, Ziya Demiroglu Y, Uncu H, Colakoglu S, Arslan H. A comparative analysis of tuberculous, brucellar and pyogenic spontaneous spondylodiscitis patients. *J Infect* 2007; 55: 158-163.
- Shi QN, Qin HJ, Lu QS, Li S, Tao ZF, Fan MG, et al. Incidence and warning signs for complications of human brucellosis: a multi-center observational study from China. *Infect Dis Poverty* 2024; 13: 18. DOI: 10.1186/s40249-024-01186-4.
- Sawafi LA, Tai AA, Reesi MA, Subhi MA, Busaidi MA, Abri SA, Waili BA. Brucellosis in Omani children: a multicenter experience over 15 years. *Ann Saudi Med* 2023; 43: 380-385.
- Solera J, Lozano E, Martínez-Alfaro E, Espinosa A, Castillejos ML, Abad L. Brucellar spondylitis: review of 35 cases and literature survey. *Clin Infect Dis* 1999; 29: 1440-1449.
- Lu YP, Qiu WQ, Zhang T, Cheng QX, Wang YZ, Chen L, et al. Epidemiology and laboratory testing of *Brucella* spondylitis. *Sci Rep* 2024; 14: 26345. DOI: 10.1038/s41598-024-77391-w.
- Gou L, Yang Y, Li J, Cai L, Xing W, Liu W, et al. MRI findings and classification of brucella spondylitis: a China multicenter study. *Eur J Med Res* 2024; 29: 469. DOI: 10.1186/s40001-024-02011-2.
- Chelli Bouaziz M, Ladeb MF, Chakroun M, Chaabane S. Spinal brucellosis: a review. *Skeletal Radiol* 2008; 37: 785-790.
- Tali ET, Koc AM, Oner AY. Spinal brucellosis. *Neuroimaging Clin N Am* 2015; 25: 233-245.
- Duarte RM, Vaccaro AR. Spinal infection: state of the art and management algorithm. *Eur Spine J* 2013; 22: 2787-2799.
- James SLJ, Davies AM. Imaging of infectious spinal disorders in children and adults. *Eur J Radiol* 2006; 58: 27-40.
- Wang J, Deng L, Ding Z, Zhang Y, Zhang Y, Li K, et al. Comparative study on the efficacy of two perioperative chemotherapy regimens for lumbar brucellosis. *Drug Des Devel Ther* 2023; 17: 3523-3536.
- Haripriya S, Malhotra S, Gadepalli R, Tak V, Kumar B. Unveiling neurobrucellosis: a case report emphasizing early diagnosis for better outcomes. *Access Microbiol* 2024; 6: 000705.v3. DOI: 10.1099/acmi.0.000705.v3.
- Al-Sous MW, Bohlega S, Al-Kawi MZ, Alwatban J, McLean DR. Neurobrucellosis: clinical and neuroimaging correlation. *AJNR Am J Neuroradiol* 2004; 25: 395-401.
- Jafari E, Togha M, Salami Z, Rahman N, Alamian S, Kheradmand JA. Seronegative brucella meningitis diagnosed by CSF PCR: report on seven cases. *BMC Infect Dis* 2024; 24: 1157. DOI: <https://doi.org/10.1186/s12879-024-10022-x>
- Yazdi NA, Moosavi NS, Alesaeidi S, Salahshour F, Ghaemi O. Diffuse neurobrucellosis of cerebellum, brainstem, spinal cord, and cauda equina: a case report and literature review. *J Radiol Case Rep* 2022; 16: 1-9.
- De la Peña-Sosa G, Cabello-Hernández AI, Gómez-Ruiz RP, Gómez-Sámano MA, Gómez-Pérez FJ. Pituitary abscess causing panhypopituitarism in a patient with neurobrucellosis: case report. *AACE Clin Case Rep* 2024; 10: 10-13.
- Alhatou M, Joudeh AI, Alhatou A, Ghamoodi M. Neurobrucellosis complicated by primary pyogenic ventriculitis: a case report. *Oxf Med Case Reports* 2024; 2024: 28-30.
- Fu XW, Bi Y, Wei JL, Qi M, Zhu L, Pu Y, et al. Differences in haematological and imaging features of lumbar spine fungal and *Brucella* infections. *Infect Drug Resist* 2024; 17: 4349-4357.
- Wang W, Fan Z, Zhen J. MRI radiomics-based evaluation of tuberculous and brucella spondylitis. *J Int Med Res* 2023; 51: 3000605231195156. DOI: 10.1177/03000605231195156.
- Chen J, Guo X, Liu X, Sheng Y, Li F, Li H, et al. Differentiation of tuberculous and brucellar spondylitis using conventional MRI-based deep learning algorithms. *Eur J Radiol* 2024; 178: 111655. DOI: 10.1016/j.ejrad.2024.111655.